Available online at www.sciencedirect.com
SCIENCE DIRECT®
Journal of Sound and Vibration 297 (2006) 200–214
JOURNAL OF SOUND AND VIBRATION
www.elsevier.com/locate/jsvi

Two-step B-splines regularization method for solving an ill-posed problem of impact-force reconstruction

Fergyanto E. Gunawan[a,*], Hiroomi Homma[b], Yasuhiro Kanto[a]

[a] *Mechanical Engineering Department, Toyohashi University of Technology, Tempaku-cho, 1-1 Hibarigaoka, Toyohashi 441-8580, Japan*
[b] *International Cooperation Center for Engineering Education Development, 1-1 Hibarigaoka, Toyohashi University of Technology, Toyohashi 441-8580, Japan*

Received 25 July 2005; received in revised form 8 February 2006; accepted 20 March 2006
Available online 2 June 2006

Abstract

This paper presents a new method to accurately solve an ill-posed problem of the impact-force reconstruction. The method utilizes B-splines to approximate and to regularize the impact-force profile. The method computes the optimal solution in two steps: the first step estimates the global profile of the impact-force, and the second step refines the force obtained in the first step. The method provides a more accurate solution because it incorporates more prior information than existing methods. Three numerical experiments presented in this paper demonstrate effectiveness of the method.

1. Introduction

An accurate characterization of the input force experienced during operation is vital in a structural reliability analysis. In common practice, the characterization of the input force utilizes a force transducer that is positioned in the load transfer path. On many circumstances, such as a high-speed impact of a small particle onto a structure, it is difficult to apply such a technique.

Another technique that has been widely used for the impact-force reconstruction is based on an inverse analysis. The inverse analysis infers the impact-force from the data of the elastic response. The method overcomes the difficulties arising in the direct measurement technique, although it still encounters other difficulties associated with the numerical instability and the solution accuracy.

Mathematically, the inverse analysis for the impact-force reconstruction is to solve a deconvolution problem. In many cases, the deconvolution results in an ill-posed problem in which the data noise strongly affects the solution accuracy. Therefore, it is difficult to obtain an accurate solution for such problems.

There are a number of publications dealing with the impact-force reconstruction problems. Doyle [1], Martin and Doyle [2], and Inoue [3] reconstructed the impact-force profile by using the spectral analysis. Their methods utilize the convolution theorem that expresses the time domain deconvolution as a simple division in the frequency domain. The frequency domain division is easy to compute, but the obtained result is sensitive

*Corresponding author. Tel.: +81 532 44 6939; fax: +81 532 44 6935.
E-mail address: gunawan@mech.tut.ac.jp (F.E. Gunawan).

0022-460X/$ - see front matter
doi:10.1016/j.jsv.2006.03.036

to the data noise and the numerical singularity. To avoid the numerical singularity, Martin and Doyle introduced a small random noise to the denominator of the equation. Inoue compared various deconvolution formulations to find one, which is less sensitive to the data noise. In addition, Inoue also minimized the noise by the data averaging.

Later on, Inoue [4,5], Adams and Doyle [6], Jacquelin et al. [7], and Liu and Sheppard [8] adopted a more systematic approach of the singular value decomposition (SVD) method. Inoue [4] utilized the SVD to locate the small singular values affected by the noise and those small singular values were eliminated in computation of the frequency response function. The Tikhonov's formulation and the SVD solution method have also been widely used as an effective method for solving the ill-posed inverse problems. For instance, Inoue [5], Adams and Doyle [6], Jacquelin et al. [7], and Liu and Sheppard [8] adopted the method to solve the reconstruction problems of harmonic and non-harmonic force profiles.

The Tikhonov's formulation incorporates a regularization parameter that controls the smoothness of the solution. The regularization parameter plays a significant role in the solution accuracy; therefore, it must be evaluated accurately. Many methods have been proposed to determine the regularization parameter. Inoue [5], Adams and Doyle [6], and Jacquelin et al. [7] utilized the L-curve method, while Liu and Sheppard [8] utilized the Morozov's discrepancy principle. In addition to the L-curve method, Jacquelin et al. [7] also utilized the generalized cross validation method.

A major drawback of the Tikhonov-SVD method is the expensive computational cost of the SVD. Therefore, the method is only suitable for small-scale inverse problems. For large-scale reconstruction problems of impact-force profile, the present authors [9] adopted an iterative regularization method of the conjugate-gradient least-square fast Fourier transformation (CGLS-FFT) method. The solutions obtained by the method was compared with that of the Tikhonov-SVD-L-curve method and it was found that the solution of the CGLS-FFT method is more accurate.

Although the CGLS-FFT method provides a better solution than the Tikhonov-SVD-L-curve method, the estimation error is still large, in order of 10% or more. The authors observed that the accuracy of those methods mainly worsens during the unloading stage. On the unloading stage, the estimated impact-force tends to oscillate, while the exact impact-force is smoothly damped down.

The Fourier analysis and the SVD use sine and cosine functions that oscillate for all time. Thus the obtained solution based on both the methods tends to oscillate. Such methods provide an accurate solution if the force is periodic as demonstrated by Liu and Sheppard [8].

In this paper, the authors intend to propose a new method that is superior in accuracy of the solution. Instead of a harmonic function, the new method utilizes a spline function. The spline function has high flexibility as compared to a harmonic function such as the sine and cosine; and can be utilized to approximate a harmonic and a transient profiles.

In the ill-posed inverse problems, the noise tends to increase the solution size. To minimize the noise effect on the solution, the Tikhonov's formulation incorporates prior information that the solution should have a minimum size. A more accurate solution should be obtained if more prior information is incorporated. The spline function is not only flexible but can also easily take into account the prior information.

This paper is organized as follows: In Section 2, the cubic spline is described briefly. In Section 3, the implementation of the B-splines function approximation to the inverse problem of the impact-force reconstruction is explained in detail. In Section 4, the present scheme is applied to the impact-force reconstruction problems of a single degree of freedom (sdof) system and a lateral impact of a circular plate. Section 5 summarizes the present method and its advantages.

2. Cubic spline

De Boor [10] and Dierckx [11] provide a detail exposition of the spline. This section only presents the necessary formulas related to the present development.

The impact-force profile is divided into several small intervals, and at each interval, a segment of the impact-force profile is approximated with a polynomial function. On the entire domain, a composite of the polynomial function constructs the impact-force profile. Fig. 1 shows the typical impact-force profile constructed by a composite of four low order polynomials.

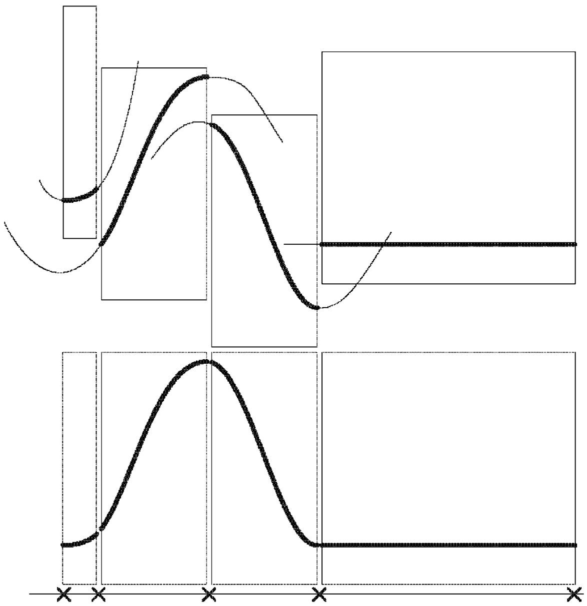

Fig. 1. A composite of four polynomials constructs a spline that approximates a typical profile of the impact-force. The symbol × denotes the knot location.

Consider a domain of $I = [a, b]$ divided into $n-1$ subintervals as $a = \lambda_1 \leqslant \lambda_2 \leqslant \cdots \leqslant \lambda_n = b$. We define a function $s(t)$ as a cubic spline on the domain if the function satisfies conditions: (i) on an interval $[\lambda_j, \lambda_{j+1}]$, $s(t)$ is a polynomial of degree 3 at most, and (ii) the function $s(t)$ and its first and second derivatives are all continuous on the domain. The cubic spline is widely used because it gives a good compromise between efficiency—computation time and memory requirements—and quality of the fit [11].

The abscissas λ_j that called nodes or knots of the spline control the curvature of the spline. A high gradient of the impact-force profile requires many knots in a short spacing. Fig. 1 shows that at least five knots are required for approximating of a simple impact-force profile.

On the jth interval, a cubic polynomial $p(t)$ can be written as

$$p_j(t) = c_{1,j} + c_{2,j}t + c_{3,j}t^2 + c_{4,j}t^3. \tag{1}$$

Conte and de Boor [12] pointed out that a Newton form of Eq. (1) is more robust and less sensitive to the round-off error:

$$p_j(t) = c_{1,j} + c_{2,j}(t - \lambda_j) + c_{3,j}(t - \lambda_j)^2 + c_{4,j}(t - \lambda_j)^3. \tag{2}$$

Four boundary conditions are required to obtain unknown coefficients $c_{i,j}, \quad i = 1, \ldots, 4$. For the data $s(\lambda_j)$ at the knot λ_j, de Boor [10] shows that those constants can be computed by

$$c_{1,j} = p_j(\lambda_j) = s(\lambda_j), \tag{3}$$

$$c_{2,j} = p_j'(\lambda_j) = m_j, \tag{4}$$

$$c_{3,j} = \frac{p_j''(\lambda_j)}{2} = \frac{[\lambda_j, \lambda_{j+1}]s - m_j}{\Delta\lambda_j} - c_{4,j}\Delta\lambda_j, \tag{5}$$

and

$$c_{4,j} = \frac{m_j + m_{j+1} - 2[\lambda_j, \lambda_{j+1}]s}{(\Delta\lambda_j)^2}. \tag{6}$$

where m_j is the slope at λ_j. The choice of the slopes $(m_j)_1^n$ differentiates piecewise cubic interpolation schemes. The term $[\lambda_i, \ldots, \lambda_{i+k}]s$ denotes the kth divided difference of the function s at sites $\lambda_i, \ldots, \lambda_{i+k}$ that computed by

$$[\lambda_i, \ldots, \lambda_{i+r}]s = \frac{s^{(r)}(\lambda_i)}{r!}, \tag{7}$$

for $\lambda_i = \lambda_{i+r}$, and it is computed by

$$[\lambda_i, \ldots, \lambda_{i+r}]s = \frac{[\lambda_{i+1}, \ldots, \lambda_{i+r}]s - [\lambda_i, \ldots, \lambda_{i+r-1}]s}{\lambda_{i+r} - \lambda_i}, \tag{8}$$

for $\lambda_i \neq \lambda_{i+r}$.

For the cubic spline interpolation, the free slopes $m_2, \ldots, m_{n-1}$ are determined from the condition that s should be twice continuously differentiable, that is, that s has also a continuous second derivative. This gives the condition that, for $j = 2, \ldots, n-1$,

$$p''_{j-1}(\lambda_j) = p''_j(\lambda_j), \tag{9}$$

or

$$2c_{3,j-1} + 6c_{4,j-1}\Delta\lambda_{j-1} = 2c_{3,j}, \tag{10}$$

or

$$\frac{2([\lambda_{j-1}, \lambda_j]s - m_{j-1})}{\Delta\lambda_{j-1}} + 4c_{4,j-1}\Delta\lambda_{j-1} = \frac{2([\lambda_{j-1}, \lambda_j]s - m_j)}{\Delta\lambda_j} + 4c_{4,j}\Delta\lambda_j, \tag{11}$$

leading to the linear system equation

$$m_{j-1}\Delta\lambda_j + m_j 2(\Delta\lambda_{j-1} + \Delta\lambda_j) + m_{j+1}\Delta\lambda_{j-1} = b_j := 3(\Delta\lambda_j[\lambda_{j-1}, \lambda_j]s + \Delta\lambda_{j-1}[\lambda_j, \lambda_{j+1}]s). \tag{12}$$

For given boundary slopes m_1 and m_n, Eq. (12) becomes a tridiagonal linear system of $n-2$ equations for the $n-2$ unknowns $m_2, \ldots, m_{n-1}$ which is strictly row diagonally dominant that can be solved by Gauss elimination without pivoting [10]. In this paper, we adopt Thomas algorithm—a special form of the Gauss elimination—for solving Eq. (12).

The function $s(t)$ can also be expressed in term of B-splines $N_i(t)$:

$$s(t) = \sum_{i=-3}^{n} c_i N_i(t), \tag{13}$$

where the B-splines $N_i(t)$ is the cubic spline with the active knots $\lambda_i, \ldots, \lambda_{i+4}$. The normalized cubic B-splines $N_i(t)$ can be explicitly computed by

$$N_i(t) = (\lambda_{i+4} - \lambda_i) \sum_{j=0}^{4} \frac{(\lambda_{i+j} - t)^3}{\prod_{l=0, l\neq j}^{4} (\lambda_{i+j} - \lambda_{i+1})}. \tag{14}$$

3. Application of B-splines for solving ill-posed problems of force reconstruction

For a linear elastic structure, the time domain convolution integral equation relates an applied impact-force $f(t)$ to an induced elastic response $e(t)$. The equation can be written as

$$\int_0^t h(t-\tau) f(\tau) = e(t), \tag{15}$$

where $h(t)$ denotes an impulse response function which is a complete characterization of the dynamic behavior of a structure. To obtain $f(t)$, one should inversely solve Eq. (15) for given data $e(t)$ and $h(t)$. Solving Eq. (15) for $f(t)$ is called the deconvolution.

For the impact-force inverse problems, the deconvolution leads to an ill-posed problem in sense of the second and third Hadamard's criteria that the noise in the data tend to dominate the solution and a small change in the data produces a significant change in the solution. A numerical regularization is necessary to accurately solve such a problem.

To numerically solve Eq. (15), the equation must be discretized. The Rieman's approximation of Eq. (15) can be expressed as

$$\sum_{k=0}^{N-1} h(i-k)f(k) = e(i), \quad \text{for} \quad i = 0, \ldots, N-1, \tag{16}$$

where $f(i)$ is the impact-force at time $t_i = i \cdot \Delta t$, and Δt is the sampling time. The impulse response function $h(i)$ and elastic response $e(i)$ adopt the same convention. Eq. (16) is written in the matrix-vector form as

$$\mathbf{Hf} = \mathbf{e}, \tag{17}$$

where **H** is a convolution matrix that has Toeplitz-circulant structure:

$$\mathbf{H} = \begin{bmatrix} h(t_0) & h(t_{N-1}) & \cdots & h(t_2) & h(t_1) \\ h(t_1) & h(t_0) & \cdots & h(t_3) & h(t_2) \\ \vdots & \vdots & \ddots & \vdots & \vdots \\ h(t_{N-2}) & h(t_{N-3}) & \cdots & h(t_0) & h(t_{N-1}) \\ h(t_{N-1}) & h(t_{N-2}) & \cdots & h(t_1) & h(t_0) \end{bmatrix}. \tag{18}$$

The convolution matrix has size of $N \times N$. The vectors **e** and **f** in Eq. (17) represent $e(i)$ and $f(i)$, respectively.

The noise in the data **e** propagates to the estimated impact-force **f** by a factor of the condition number of the matrix **H**. The impact-force inverse problems discussed in this paper are having the condition number in order of 1.0E+04 to 1.0E+05.

In the present method, we approximate the impact-force **f** with a linear combination of the B-splines. Thus the impact-force can be written as

$$\mathbf{f} = \mathbf{Nw}, \tag{19}$$

where the matrix **N** consists of M B-splines and the vector **w** consists of weightings of B-splines. A non-decreasing order of the knot sequence $\boldsymbol{\lambda}$ defines the B-splines. The number of the knots $\#\boldsymbol{\lambda}$ is related to the number of the cubic B-splines M by $M + 3 = \#\boldsymbol{\lambda}$. Utilization of the B-splines approximation function reduces the impact-force inverse problem to a problem of determining the knot sequence $\boldsymbol{\lambda}$ and the weighting **w** of B-splines.

3.1. Solution of a linear least-square problem

Substituting Eq. (19) into Eq. (17) provides

$$\mathbf{H}(\mathbf{Nw}) = \mathbf{e}, \tag{20}$$

that should be solved by means of the least-square method, because the elastic response data **e** contains the noise.

The matrix **N** consists of some sequences of the B-splines, therefore **N** is a banded matrix. The QR decomposition method that decomposes a matrix into an orthogonal matrix and an upper triangular matrix can efficiently solve the above problem.

Although the matrix **H** is an ill-posed matrix, but the matrix **N** has strong diagonal entities, therefore, the matrix **A**, a product of **H** and **N**, will be a well-posed matrix. Many direct or iterative solution methods can solve Eq. (20) accurately.

In this paper, the Q-less QR decomposition and the one step of iterative refinement solution method are adopted. The method computes **w** in the following steps:

Firstly, we decompose the matrix **A** by the QR decomposition into two matrices as

$$\mathbf{A} = \mathbf{QR}, \tag{21}$$

where **Q** is an orthogonal matrix and **R** is an upper triangular matrix. The first approximation of the solution **w** is obtained by

$$\mathbf{w} = \mathbf{R}^{-1}(\mathbf{R}^{-1}(\mathbf{A}^{\mathrm{T}}\mathbf{e})). \tag{22}$$

Secondly, the one step iterative refinement is applied to improve the solution accuracy by, sequentially:

$$\mathbf{r} = \mathbf{e} - \mathbf{A}\mathbf{w}, \tag{23}$$

$$\boldsymbol{\varepsilon} = \mathbf{R}^{-1}(\mathbf{R}^{-1}(\mathbf{A}^{\mathrm{T}}\mathbf{r})) \tag{24}$$

and

$$\mathbf{w} = \mathbf{w} + \boldsymbol{\varepsilon}. \tag{25}$$

Substitution of **w** into Eq. (19) provides the estimated impact-force **f**.

3.2. Regularization

Generally, ill-posed inverse problems require a numerical regularization to minimize the data error, the discretization error and the round-off error. Two widely used regularization methods are the Tikhonov regularization and the iterative regularization. In the Tikhonov regularization, the regularization parameter is explicitly computed and determined as a part of the solution process. The computation has to be repeated many times to obtain the optimal regularization parameters that minimize the noise and the residue. Several methods are proposed to compute the optimal regularization parameter. The most notable ones are the L-curve and the generalized cross validation (GCV) methods. Hansen [13] reported that the L-curve method is more robust than the GCV method, but it tends to produce a regularization parameter that brings slightly over smooth solution.

The L-curve is a plot of the residue norm against the regularized solution norm. In the L-curve, the optimal solution lies at the curve corner. It is shown that if the data of **h** and **e** are normalized with their Euclidian norm, the corner can be accurately located by [9]:

$$\min_{\mathbf{f}} ||\mathbf{H}\mathbf{f} - \mathbf{e}||_2^2 + \|\mathbf{f}\|_2^2, \tag{26}$$

where **f** is a regularized solution. The above criterion is similar to a criterion presented by Hanke [14] that the regularization should be chosen in such a way that the residual and the errors in the data are essentially the same size.

Essentially, the regularization parameter in the Tikhonov method suppresses the fluctuation in the solution. On the other side, the fluctuation of a spline can be controlled by its knots. Therefore when B-splines function is used to approximate the impact-force profile, the number and the position of the knots control the smoothness of the profile. In other words, the knots regularize the solution.

The present method computes the optimal solution in two steps. In the first step, the knots are coarsely distributed to the entire domain of the analysis to capture the loading and the unloading stages of the impact-force. The number of the knots is varied, and then for each knots configuration, the impact-force is computed and also the above criterion. The configuration of the knots that provide a lowest value of Eq. (26) is selected for the second step analysis.

Based on the result of the first step analysis, one can establish the loading and the unloading stages. In the second step analysis, the knots along the unloading stage are deleted and new knots are inserted along the loading stage. The number of the inserted knots along the loading stage is also varied to minimize Eq. (26).

4. Numerical studies

Ref. [9] shows the iterative regularization of the CGLS-FFT method that minimizes Eq. (26) provides a reasonable accurate solution. For this reason, the solution by the present method will be compared to the CGLS-FFT solution. The comparison will be made quantitatively by way of the relative estimation error:

$$\tilde{\mathbf{f}} = \frac{\mathbf{f}_{\text{Exact}} - \mathbf{f}_{\text{Estimated}}}{\mathbf{f}_{\text{Exact}}} \times 100\%. \quad (27)$$

4.1. Simple impact-force acting on an sdof

Consider an sdof system subjected to an impact-force $f(t)$. The system consists of a mass, a spring and a dashpot. The impulse response function of the system can be expressed as

$$h(t) = \frac{1}{m\omega_d} \mathrm{e}^{-\xi\omega_n t} \sin(\omega_d t), \quad (28)$$

where ω_n and ω_d denote the circular natural and the circular damped frequencies. Both the parameters can be computed by

$$\omega_n = \sqrt{\frac{k}{m}} = 2\pi f_n, \quad (29)$$

and

$$\omega_d = \omega_n\sqrt{1-\xi^2}. \quad (30)$$

In the present study, the following data are selected: $m = 1$ kg, $k = 1.0\mathrm{E}+11$ N/m, $\xi = 0.1$, and the final time is 100.0 μs. The analysis domain is divided into 256 points.

A convenient procedure to obtain the data for the inverse analysis is by a forward analysis. It is assumed that the impact-force $f(t)$ takes a form of a half-sine function. The elastic response $e(t)$ can be computed by convolving $f(t)$ and $h(t)$. To accommodate a measurement noise that inherently exists in the measurement process, a pseudo random noise having Gaussian distribution and variance 20% of the maximum data is superimposed to the elastic response $e(t)$.

4.1.1. First step B-splines regularization

In the first step, the knots are evenly distributed along the time-domain of the analysis. Too many knots reduces the degree of the regularization, while too few knots increases the regularization. In this step, the number of the knots is gradually increased from 5 to 30, and for each number of the knots, Eq. (20) is solved to obtain the knots weighting **w**, and then the impact-force **f** is computed. Among the obtained solutions, the solution that minimizes Eq. (26) is selected as an optimal solution.

Fig. 2 shows the optimal solution obtained by 19 knots. Those knots locations are marked with a symbol × on the figure. The figure indicates that the loading stage begins at 5.5 μs and ends at 43.9 μs.

4.1.2. Second step B-splines regularization

Fig. 2 shows the four knots; marked with □, play a crucial role as the cornerstones of the present impact-force profile. Those knots are located at 0.0, 5.5, 43.9, and 100.0 μs. The first and the end knots are required for the initial and final time of the analysis, the second and the third knots are required to capture the loading stage and no knots are required in duration 0.0–5.5 μs and 43.9–100.0 μs.

In the second step B-splines regularization method, the region of interest is along the loading stage, in this case is 5.5–43.9 μs. Similarly to the first step, 5–30 knots are gradually inserted into the region, and for each knots sequence, the weighting **w** is computed. Furthermore, the optimal solution that minimizes Eq. (26) is selected from the obtained solutions.

Fig. 3 shows the result obtained by the two-step B-splines regularization method. In the same figure, the exact and the CGLS-FFT solutions are also presented. It is clearly shown that the two-step B-splines regularization method provides a better solution than the CGLS-FFT solution. In addition to the figure, the comparison between the present method and the CGLS-FFT method is also presented in term of the relative estimation error in Table 1. The relative estimation error is computed by Eq. (27). It is seen that the two-step B-splines regularization method is twice as accurate as the CGLS-FFT method.

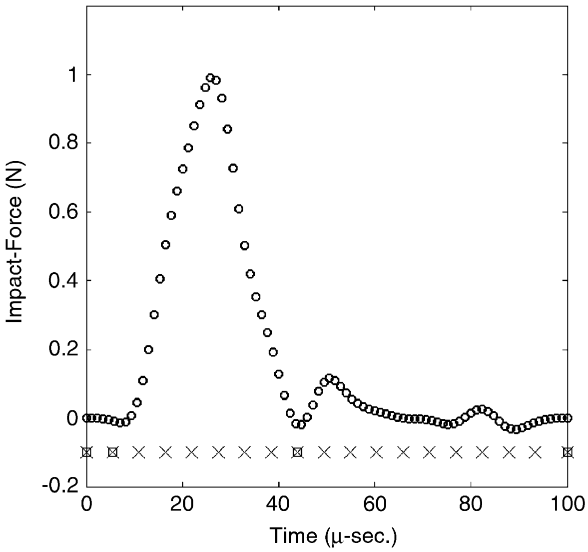

Fig. 2. The estimated impact-force by the first step B-splines regularization method and the associated knots (shown by symbol ×). The symbol □ denotes the required knots to capture the loading and the unloading stages of the impact-force profile.

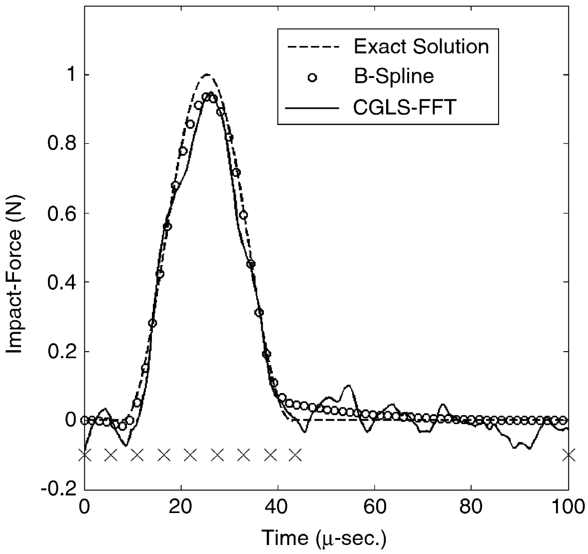

Fig. 3. The exact, the two-step B-splines, and the CGLS-FFT solutions for an sdof impact problem, and the associated knots (shown by symbol ×).

Table 1
The relative estimation errors for problems of an sdof system subjected to a simple impact-force profile, a complex impact-force profile, and a lateral impact of a circular plate

Case	Relative estimation error (%)		
	CGLS-FFT	First step B-splines	Second step B-splines
sdof with simple force	15	11	7
sdof with complex force	18	24	9
Plate bending	15	17	7

4.2. Complex impact-force acting on an sdof

Inoue et al. [4] showed that the impact-force profile could be more complex than a half-sine function. This section deals with a problem of estimating a complex impact-force profile.

To concentrate the attention on the complex impact-force profile, the study is isolated to an impact problem of the sdof system. The sdof system has the same properties as the former one. The system is subjected to a complex impact-force profile and its response that contains 20% noise is presented in Fig. 4. The impact-force is reconstructed in a similar way to that presented in Section 4.1.

Figs. 5 and 6 show the results of the estimated impact-force for the first step and the second step B-splines regularization method, respectively. Fig. 5 shows that the first estimation of the impact-force does not clearly

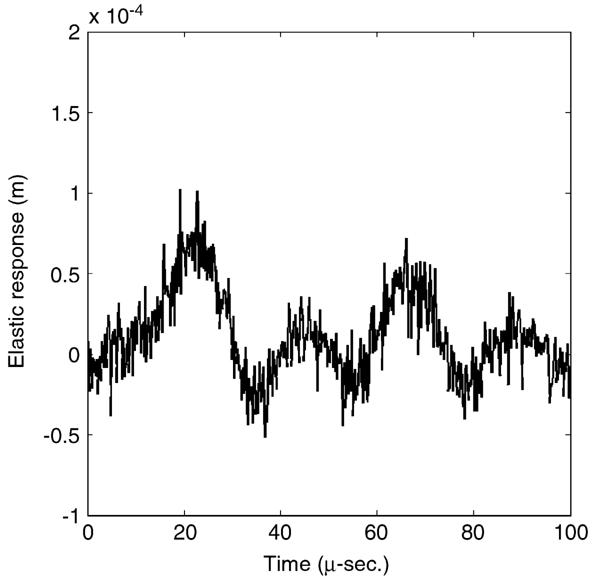

Fig. 4. The elastic response of an sdof system subjected to a complex impact-force profile.

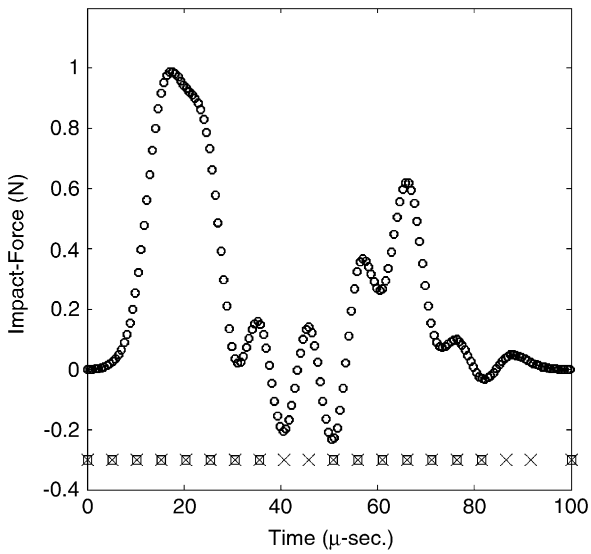

Fig. 5. The estimated impact-force by the first step B-splines method and its associated knots (shown by symbol ×) for an sdof system subjected to a complex impact-force profile.

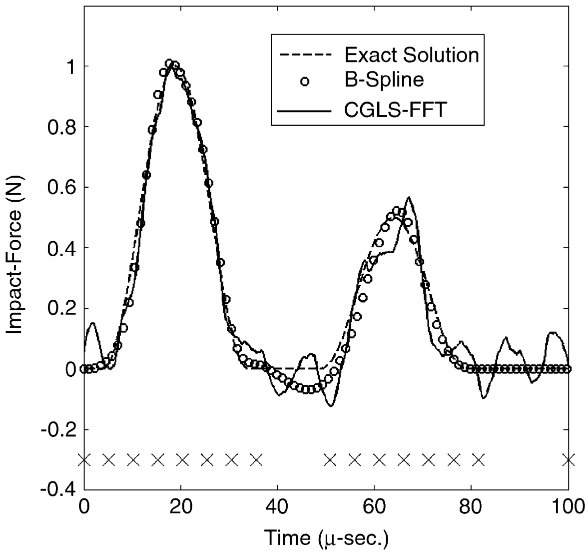

Fig. 6. The exact, the two-step B-splines, and the CGLS-FFT solutions for an sdof system subjected to a complex impact-force profile, and the associated knots (shown by symbol ×).

reveal the profile of the impact-force. The figure shows the impact-force is negative at about 40.0 and 80.0 μs. The physical restriction imposes the impact-force should be greater than zero. Since the B-splines is always greater than zero, thus the negative impact-force at those times is because of the negative weighting factors. For this reason, the four knots located at those times that the impact-force violates the physical restriction are eliminated.

Fig. 6 shows the new configuration of the knots and the associated solution of the impact-force. The figure also shows the exact impact-force that applied to the system and one that obtained by the CGLS-FFT method. The figure clearly shows the two-step B-splines regularization method produces a more accurate estimated impact-force. In addition to the figure, the comparison is also presented in Table 1 in term of the relative estimation error. The table shows the two-step B-splines method is 50% more accurate than the CGLS-FFT method.

4.3. Lateral impact of plate

The plate bending is an important basic structure. Thus, this section deals with a profile reconstruction of a lateral impact-force on a circular plate.

The plate is made of a steel material of which the Young's modulus, the Poisson's ratio and the density are 200 GPa, 0.3, and 7800 kg/m^3, respectively. The plate size is 5.0 mm in thickness and 100.0 mm in radius. The lateral impact-force is applied to the center of the front surface and the elastic response of the strain is measured at the center of the back surface. Fig. 7 shows the applied force, the boundary conditions, and the measurement point.

4.3.1. Impulse response function estimation

The inverse analysis of the impact-force reconstruction requires the data of the impulse response function and the elastic response of the plate. It is difficult to obtain the exact solution of the impulse response function for a plate subjected to an impact-force. Therefore, the impulse response function will be computed numerically.

Eq. (15) satisfies the commutative law of the convolution, hence it can also be expressed as

$$\int_0^t h(\tau)f(t-\tau)d\tau = e(t), \tag{31}$$

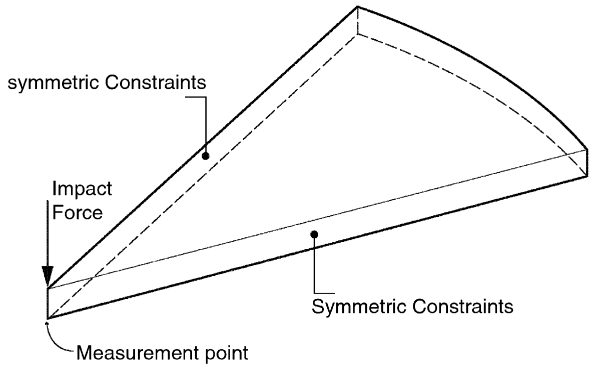

Fig. 7. A 30 degrees pie-model of a circular plate.

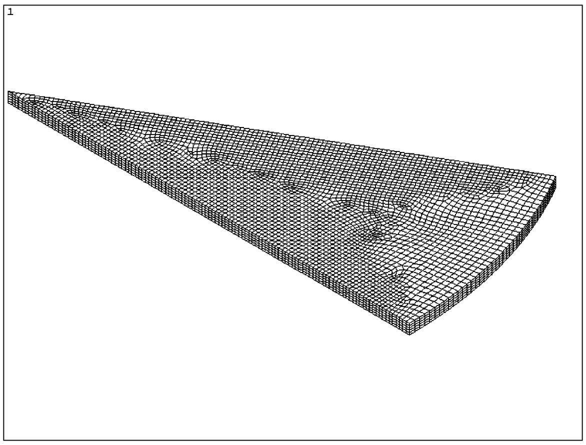

Fig. 8. The finite element mesh of a 30 degrees pie-model of the circular plate.

and in a discrete form, it can be written as

$$\mathbf{Fh} = \mathbf{e}, \tag{32}$$

where **F** is a Toeplitz-circulant matrix of the impact-force.

Eqs. (15) and (31) shows estimation problem of the impact-force and the impulse response function are the same from the mathematical viewpoint that both the problems are deconvolution. Therefore, the present method is applicable to both the problems.

To determine the impulse response function using Eq. (32), the data of the elastic response and the applied impact-force are necessary. Hence, two data sets are required to verify the two-step B-splines regularization method. The first data set is used for the calibration process to determine the impulse response function and the second data set is necessary for the impact-force estimation. Each data set consists of the data of the impact-force and its associated response. Those data are obtained from a forward analysis using the finite element method (FEM).

Fig. 8 shows a finite element mesh of a 30 degrees pie-model that consists of 20 742 nodes and 16 585 solid elements. Each element has 8 nodes and each node has 9 degree of freedoms. The analysis time is 256.0 μs that divided into 1024 time-steps. The model takes advantage of the axis-symmetry of the applied impact-force and the plate geometry. The applied impact-force takes a form of a half-sine function. Fig. 9 shows the computed elastic responses for the impact-force durations of 10.0, 20.0, 30.0, 40.0 and 50.0 μs.

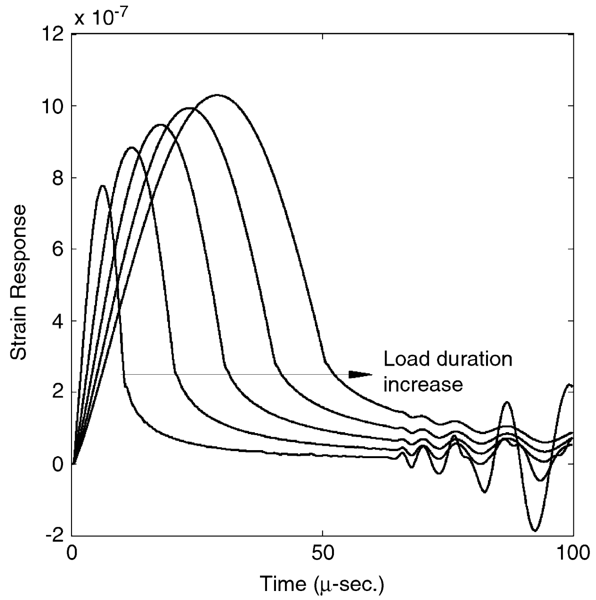

Fig. 9. The elastic responses of the circular plate subjected to an impact-force of durations of 10.0, 20.0, 30.0, 40.0 and 50.0 μs.

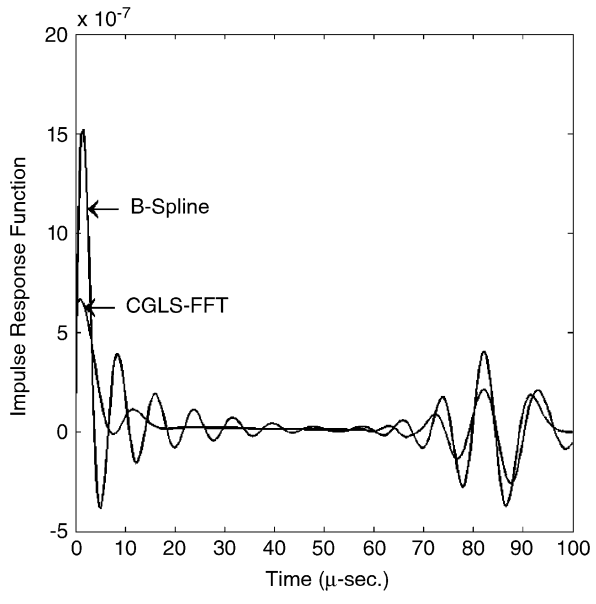

Fig. 10. The estimated impulse response function by the B-splines regularization and the CGLS-FFT methods based on the data of 10.0 μs impact duration.

For the calibration, the data set of 10.0 μs loading duration is selected, because it has a wider frequency content than the data of longer loading durations. Eq. (32) is solved for the impulse response function by the CLGS-FFT and B-splines regularization methods.

Fig. 10 presents the estimation results of the impulse response function. It is shown the B-splines regularization method provides a solution containing higher modes of vibration than a solution by the CGLS-FFT method. The optimal solution by the B-splines method is obtained by 28 knots with three knots placed at 0.0 μs and the remaining knots evenly distributed along the analysis time. Those three knots are placed to capture the high gradient of profile.

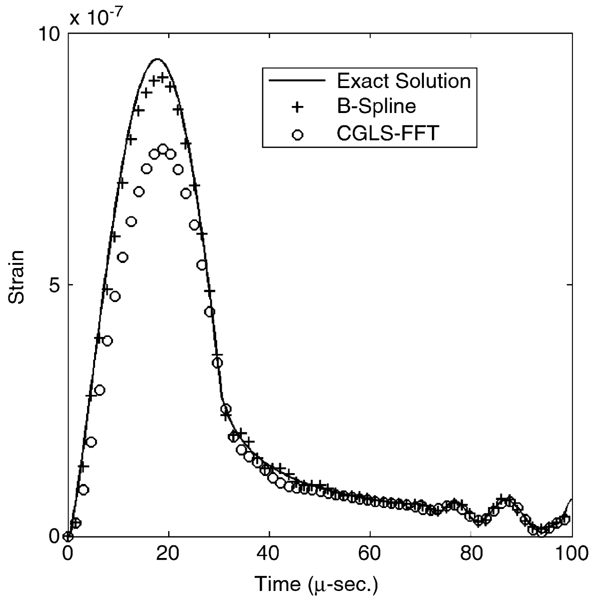

Fig. 11. The elastic responses obtained from a finite-element analysis, convolution of a 30.0 μs duration impact-force with the estimated impulse response function by the B-splines method, and convolution of the same impact-force with the estimated impulse response function by the CGLS-FFT method for case of a circular plate impact.

Theoretically, the impulse response function at time 0.0 μs is zero. This prior information can easily be incorporated into the solution by the B-splines regularization method, but not for the CGLS-FFT method. In this respect, as shown in Fig. 10, the B-splines regularization method provides a better solution.

At this stage, it is difficult to evaluate the accuracy of the estimated impulse response function, because the exact solution is not available. The accuracy is evaluated at the next stage in which the estimated impulse response function is convolved with an impact-force of the second data set of 30.0 μs loading duration to produce an estimated elastic response for the case. The elastic response has also been computed by the finite-element analysis as depicted in Fig. 9. The discrepancy between the estimated elastic response and the FEM result directly measures the accuracy of the estimated impulse response function, because the convolution is numerically stable, thus the accuracy of the estimated elastic response fully depends on the accuracy of the estimated impulse response function.

Fig. 11 presents the comparison between the convolution result and the FEM result. The figure shows that the estimated impulse response function by the B-splines method is more accurate than that of the CGLS-FFT method. Onward, the following paragraph that focuses on the impact-force reconstruction, will utilize the B-splines estimated impulse response function.

4.3.2. *Impact-force reconstruction*

A problem of the impact-force reconstruction is restated as following: for a given elastic response depicted in Fig. 11 as a solid line, and an impulse response function depicted in Fig. 10, estimate the applied impact-force.

It is well known that the ill-posed inverse problems are very sensitive to the data noise. E. Jacquelin et al. [7] pointed out that for the force reconstruction, only the noise on the elastic response affects accuracy of the estimated impact-force. For the reason, in this study only the elastic response data is superimposed with a pseudo random noise. The noise has Gaussian distribution with variance of 10% of the maximum data.

In the first step B-splines regularization method, a similar study as presented in Section 4.1.1 is performed. It should be noted that the purpose of the study is to detect the loading and unloading stages. The study reveals that 45 knots are required to capture the profile of the impact-force. Three knots are placed at the time 0.0 μs because of the high-loading rate at the time.

Fig. 12 shows the result by the first step B-splines regularization method. The figure shows that the impact-force starts at about 0.0 μs and ends at about 30.0 μs.

At the second step B-splines regularization, the attention is given to the knots distribution in the loading stage: 0.0–30.0 μs; and the number of the knots within the domain is studied. In the study, the number of the knots in the loading stage is gradually varied from 2 to 20; and for each number of the knots, the impact-force **f** and also the objective function of Eq. (26) are computed. A configuration of the knots that has lowest value of $||\mathbf{Hf} - \mathbf{e}||^2 + ||\mathbf{f}||^2$ is considered the best solution.

The best solution presented in Fig. 13 is constructed by 12 knots. The figure also shows the location of those knots.

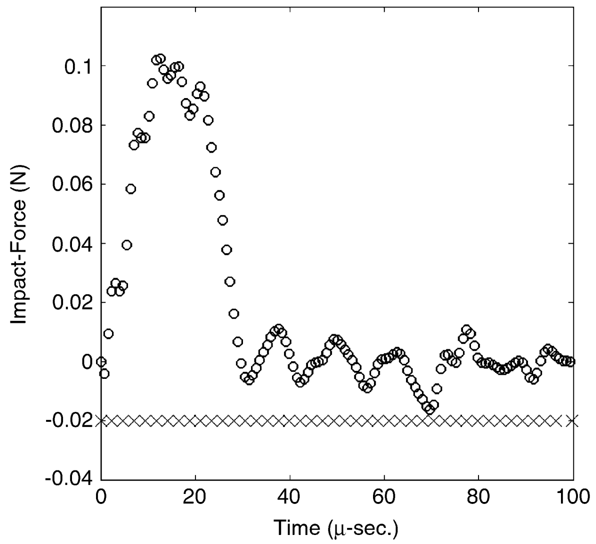

Fig. 12. The estimated impact-force by the first step B-splines regularization method and the associated knots (shown by symbol ×) for case of a circular plate impact.

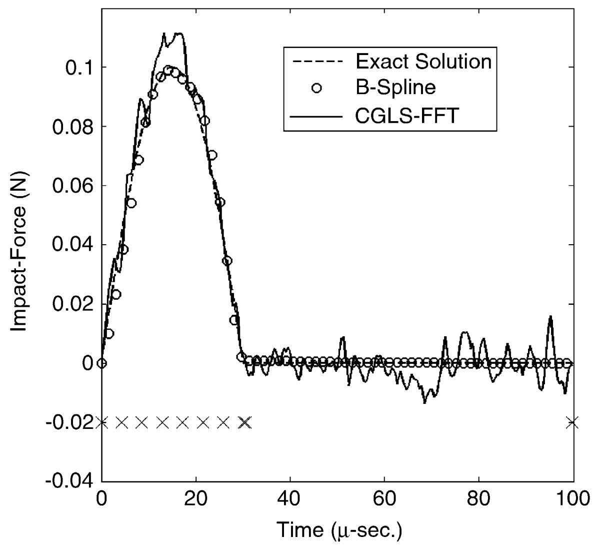

Fig. 13. The exact, the two-step B-splines, and the CGLS-FFT solutions of the impact-force for case of a circular plate, and the associated knots (shown by symbol ×).

In Table 1, a comparison between the two-step B-splines regularization and the CGLS-FFT methods is given. The table shows the present method improves the solution accuracy by a factor of more than 50%. In addition, the comparison of the estimated impact-force is also shown in Fig. 13. The figure also shows the exact impact-force that applied to the finite element model. Those comparisons suggest that the two-step B-splines method achieves an excellent estimation in the unloading stage and in the peak of the impact-force.

5. Conclusions

The two-step B-splines regularization method has been developed to solve ill-posed inverse problems in high accuracy. Unlike the Tikhonov-SVD method that approximates the solution by use of the harmonic function, the two-step B-splines method approximates the solution by use of the spline function. The spline knot is used to control the degree of the regularization.

The method takes advantages of the spline, which has flexibility in approximation of harmonic and non-harmonic profiles. In addition, the method can easily incorporate prior information of a solution into the calculation. These advantages of the spline are integrated in the two-step B-splines regularization method to obtain an accurate impact-force even for a complex force profile.

References

[1] J.F. Doyle, Determining the contact force during the transverse impact of plate, *Experimental Mechanics* 27 (1) (1987) 68–72.
[2] M.T. Martin, J.F. Doyle, Impact force identification from wave propagation responses, *International Journal of Impact Engineering* 18 (1) (1996) 65–77.
[3] H. Inoue, K. Kishimoto, T. Shibuya, T. Koizumi, Estimation of impact load by inverse analysis (optimal transfer function for inverse analysis), *JSME International Journal* 35 (4) (1992) 420–427.
[4] H. Inoue, K. Kishimoto, T. Shibuya, T. Koizumi, Estimation of impact force by an inverse analysis, *Inverse Problem in Engineering Mechanics: IUTAM Symposium, Tokyo, 1992*, Springer, Berlin, 1993.
[5] H. Inoue, K. Kishimoto, T. Shibuya, K. Harada, Regularization of numerical inversion of the Laplace transform for the inverse analysis of impact force, *JSME International Journal, Series A, Solid Mechanics and Material Engineering* 41 (4) (1998) 473–479.
[6] R. Adams, J.F. Doyle, Multiple force identification for complex structures, *Experimental Mechanics* 42 (1) (2000) 25–37.
[7] E. Jacquelin, A. Bennani, P. Hamelin, Force reconstruction: analysis and regularization of a deconvolution problem, *Journal of Sound and Vibration* 265 (2003) 81–107.
[8] Y. Liu, S. Shepard Jr., Dynamic force identification based on enhanced least squares and total least-squares schemes in the frequency domain, *Journal of Sound and Vibration* 282 (2005) 37–60.
[9] F.E. Gunawan, H. Homma, Accurate estimation of impact force by inverse analysis, *Proceedings of the Mechanical Engineering Congress*, Hokkaido, Japan, 2004.
[10] C. de Boor, *A Practical Guide to Splines*, Springer, Berlin, 2001.
[11] P. Dierckx, *Curve and Surface Fitting with Splines*, Oxford Science Publications, Oxford, 1993.
[12] S.D. Conte, C.W.D. Boor, *Elementary Numerical Analysis: An Algorithmic Approach*, third ed., McGraw-Hill Higher Education, New York, 1980.
[13] P.C. Hansen, D.P. O'Leary, The use of the L-curve in the regularization of discrete ill-posed problems, *SIAM Journal on Scientific Computing* 14 (1993) 1487–1503.
[14] M. Hanke, Iterative regularization techniques in image restoration, in: D. Colton, et al. (Eds.), *Surveys on Solution Methods for Inverse Problems*, Springer, Wien, 2000, pp. 35–52.